

## Two different ground states in K-intercalated polyacenes

Quynh T. N. Phan,<sup>1</sup> Satoshi Heguri,<sup>1,\*</sup> Hiroyuki Tamura,<sup>1</sup> Takehito Nakano,<sup>2</sup> Yasuo Nozue,<sup>2</sup> and Katsumi Tanigaki<sup>1,3,†</sup>

<sup>1</sup>WPI-Advanced Institute for Materials Research (WPI-AIMR), Tohoku University, 2-1-1 Katahira, Aoba, Sendai, Miyagi 980-8577, Japan

<sup>2</sup>Department of Physics, Graduate School of Science, Osaka University, 1-1 Machikaneyama, Toyonaka, Osaka 560-0043, Japan

<sup>3</sup>Department of Physics, Graduate School of Science, Tohoku University, 6-3 Aoba, Aramaki, Aoba, Sendai, Miyagi 980-8577, Japan

(Received 5 December 2015; revised manuscript received 28 January 2016; published 16 February 2016)

The electronic states of potassium- (K-) intercalated zigzag-type polycyclic aromatic (PLA) hydrocarbon [polyacene PLAs]  $K_x$ (PLAs) are studied for a series of the four smallest molecules: naphthalene (NN), anthracene (AN), tetracene (TN), and pentacene (PN), focusing on their 1:1 stoichiometric phases. Clear experimental differences are identified between the first group [ $K_1$ (NN) and  $K_1$ (AN)] and the second group [ $K_1$ (TN) and  $K_1$ (PN)] by magnetic, vibrational, and optical measurements. The first group is categorized as a Mott insulator with an antiferromagnetic ground state with energy of  $\sim 10$  meV, whereas the second group is classified as a band insulator via dimer formation due to the spin Peierls instability. In the latter system, the first thermally accessible triplet states are located far apart from the singlet ground states and are not detected by electron spin-resonance spectroscopy until 300 K being very different from what is observed for the hole-doped PN reported earlier. The results give a new systematic understanding on the electronic states of electron-doped PLAs sensitive to the energetic balance among on-site Coulomb repulsion, bandwidth, and the Peierls instability.

DOI: [10.1103/PhysRevB.93.075130](https://doi.org/10.1103/PhysRevB.93.075130)

### I. INTRODUCTION

A semiconducting state showing high conductivity  $1 \times 10^{-3} \Omega^{-1} \text{cm}^{-1}$  was observed in halogen-doped perylene in 1954 [1]. This has inspired many studies to search for a metallic state composed of only simple polycyclic aromatic hydrocarbon (PAH) by carrier doping. Although a real metallic behavior followed by the first discovered organic superconductor was found for sulfur- and selenium-substituted organic charge-transfer complexes later, a metallic state in carrier-doped simple PAHs has been a long-sought after scientific interest and still remains an open question.

A recent report on superconductivity in potassium- (K-) doped picene [2] and phenanthrene [3–5] suggested an intriguing argument as to whether such a real metallic state possessing a Fermi surface can be created in PAHs by electron doping. Although theoretical and experimental controversies expressing both positive [6–12] and negative opinions [13–17] had been given on the existence of such a superconducting phase, we have recently shown that these reports are not experimentally correct [16,17]. Consequently, no metallic states still exist in PAHs intercalated with alkali- and alkaline-earth metals.

Two geometrical structures can generally be considered in PAHs, armchair and zigzag types. Molecules in the latter group are generally named polyacenes (PLAs) and they are well-known organic semiconductors for applications to field-effect transistors. Figure 1 displays the molecular structures of the four smallest PLAs: naphthalene (NN), anthracene (AN), tetracene (TN), and pentacene (PN), together with a correlation between bandwidth ( $W$ ) derived from the lowest unoccupied molecular orbitals (LUMOs) and the number of benzene rings [18]. In the past, many experimental approaches

on intercalation with alkali and alkaline-earth elements were performed by focusing on TN and PN. In electron-doped TN or PN thin films with the 1:1 stoichiometry, a Mott insulating state was suggested in the past based on its electrical transport measurements as well as photoemission studies [19–22]. On the other hand, iodine- (I-) intercalated PN in bulk with a similar stoichiometry from the viewpoint of hole carriers with the opposite charge state was reported to produce an electronic ground state of a singlet, and its thermally accessible singlet-triplet excitation of localized electrons was suggested from the temperature dependence of spin susceptibility [23]. We recently reported from magnetic, Raman, and optical measurements that a Mott insulating ground state is produced in  $K_1$ (AN) of the 1:1 stoichiometric intercalation due to the large on-site Coulomb repulsion energy ( $U$ ) in comparison with  $W$  [24]. A debate has still been continuing as to whether the electronic ground states of PLA with a half-filled band are either a Mott insulator or another electronic state.

In the present paper, we report unambiguous evidence that the ground states of the four smallest PLAs intercalated with K in the 1:1 stoichiometry is intriguingly different between the smaller group (NN,AN) and the larger group (TN,PN). The former group shows Mott insulating ground states, but on the other hand the latter one possesses singlet ground states via dimerization due to the spin Peierls instability as an energetically more stable state. In the latter group, however, the energy gap between the singlet and the thermally excited triplet state is located energetically much higher than the energy at room temperature, and accordingly the thermally excited triplet is missing in magnetic observations. The ground states of  $K_1$ (PLAs) change by a sensitive balance in the energetic competition among  $U$ ,  $W$ , and the formation of a dimer as a consequence of a spin Peierls instability. Clear evidence showing different electronics states is given by superconducting quantum interference device (SQUID) measurements as well as vibrational and optical spectroscopic data, and reasonable interpretations of these experimental data are provided based on first-principles calculations.

\*Author to whom correspondence should be addressed: [heguri@m.tohoku.ac.jp](mailto:heguri@m.tohoku.ac.jp)

†[tanigaki@sspn.sphys.tohoku.ac.jp](mailto:tanigaki@sspn.sphys.tohoku.ac.jp)

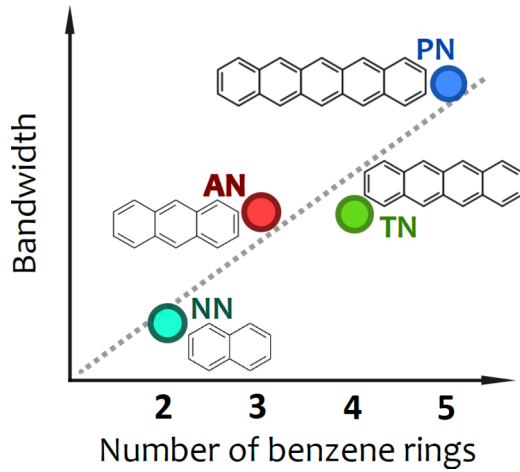


FIG. 1. Schematic of the LUMO bandwidth against a number of benzene rings for the first four PLAs.

## II. EXPERIMENT

The major synthetic problems of intercalated PLA were the fact that PLAs are volatile organic compounds and therefore were difficult in controlling the stoichiometry. Furthermore a bad diffusion process of K into organic materials induces various metastable phases, so-called polymorphic phases. In order to improve the reaction conditions, nominal 1:1 stoichiometric intercalation compounds between K and PLAs were prepared by modified solid-state reactions, which involve careful grinding for mild intercalation reactions at room temperature by employing the lower annealing temperature [24,25]. It is important to note that reactions occur only by grinding even at room temperature. Powder x-ray diffraction (XRD) of pristine and intercalated samples was measured at the BL02B2 beam port in SPring-8. Raman spectroscopy was performed at room temperature using a RENISHAW inVia Reflex spectrometer equipped with a single monochromator and a CCD detector with an excitation wavelength of 785 nm for NN and AN and 633 nm for TN. The samples were sealed into soda-glass capillaries in an argon atmosphere for both XRD and Raman measurements. Diffusive reflection spectra measurements were carried out in high quality quartz tubes at room temperature by using UV-vis-NIR and Fourier transform IR spectrometers. A SQUID spectrometer (Quantum Design with a 7-T magnet) was used to measure the electronic properties of K-intercalated PLAs. The samples for the SQUID measurements were sealed in quartz tubes filled with helium gas. The electronic structures of the PLAs were calculated using *ab initio* calculations, and the dimers of the PLA monoanions  $[(\text{PLA})^{1-}]_2$  were considered as a model system. Although the positions of K cations in the  $\text{K}_1(\text{PLA})$  crystals are not fully understood, the configurations of PLA molecules were not supposed to be significantly different from those of pristine PLA. Multireference second-order perturbation theory (MRMP2) was employed for properly describing the strongly correlated electron systems, and the general atomic and the molecular electronic structure system (GAMESS) code was used for the *ab initio* calculations [26].

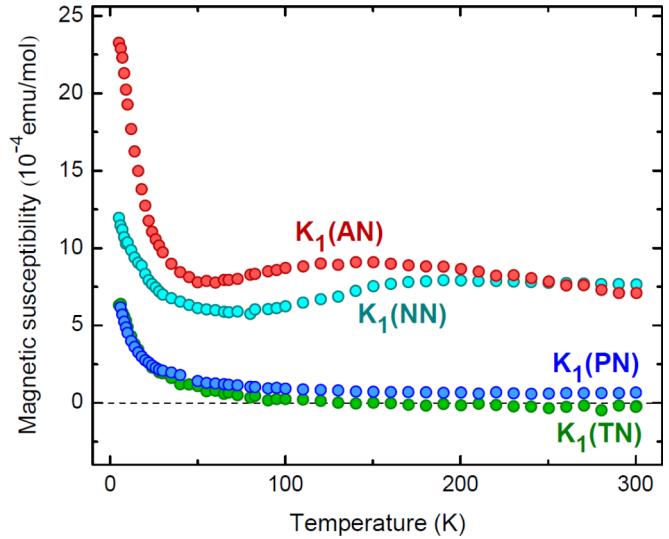


FIG. 2. Temperature dependence of the magnetic susceptibilities of  $\text{K}_1(\text{NN})$ ,  $\text{K}_1(\text{AN})$ ,  $\text{K}_1(\text{TN})$ , and  $\text{K}_1(\text{PN})$ .

## III. RESULTS AND DISCUSSION

### A. Magnetic properties

The temperature dependence of magnetic susceptibilities ( $\chi$ ) of  $\text{K}_1(\text{NN})$ ,  $\text{K}_1(\text{AN})$ ,  $\text{K}_1(\text{TN})$ , and  $\text{K}_1(\text{PN})$  was studied by SQUID as shown in Fig. 2. As displayed in this figure,  $\text{K}_1(\text{TN})$  and  $\text{K}_1(\text{PN})$  showed a very different temperature evolution of  $\chi$  from those of  $\text{K}_1(\text{NN})$  and  $\text{K}_1(\text{AN})$ . As reported earlier,  $\text{K}_1(\text{AN})$  showed an interaction energy ( $|J/k_B|$ ) of 140 K, and the ground state is a Mott insulator under a condition of  $U/W > 1$  [24].  $\text{K}_1(\text{NN})$  showed a similar pronounced hump, which shifted to a higher temperature than that of  $\text{K}_1(\text{AN})$ . This is evidence that the Mott insulator is the ground state for both  $\text{K}_1(\text{NN})$  and  $\text{K}_1(\text{AN})$ . More supporting evidence is inferred later from optical and Raman spectroscopic experiments.

On the other hand, both  $\text{K}_1(\text{TN})$  and  $\text{K}_1(\text{PN})$  showed very small magnetic susceptibilities which are far below the values of  $\text{K}_1(\text{NN})$  and  $\text{K}_1(\text{AN})$ . Temperature dependences of their magnetic susceptibilities were fitted by employing the Curie law  $\chi(T) = C/T$  [Eq. (1)], where  $C = n\mu_B^2/k_B$  is the Curie constant from which the number of spins ( $n$ ) was evaluated to be 0.006 and 0.01 spin/molecule for  $\text{K}_1(\text{TN})$  and  $\text{K}_1(\text{PN})$ , respectively. These small  $n$  values can be ascribed to the defects in the crystal.

Considering the extremely small magnetic susceptibility observed for  $\text{K}_1(\text{TN})$  and  $\text{K}_1(\text{PN})$ , they are neither metals nor Mott insulators. Two scenarios can be considered as the reason for the small  $n$  observed for  $\text{K}_1(\text{TN})$  and  $\text{K}_1(\text{PN})$ . The first is that the formed species are a divalent state, such as  $\text{PLA}^{2-}[\text{K}_2(\text{PLAs})]$  instead of a monovalent state, such as  $\text{PLA}^{1-}[\text{K}_1(\text{PLAs})]$ . In such a case, two electrons are transferred to one TN or PN molecule from two K intercalants, and therefore the LUMO-derived band is fully occupied by a pair of up and down spins as the singlet ground state. It is noted here that a single band picture is necessary for having such a divalent valence state because a degenerate band, such as the triply degenerate  $t_{1u}$ -derived band in  $\text{C}_{60}$ , gives a more complex situation [27]. The second scenario is a spin Peierls

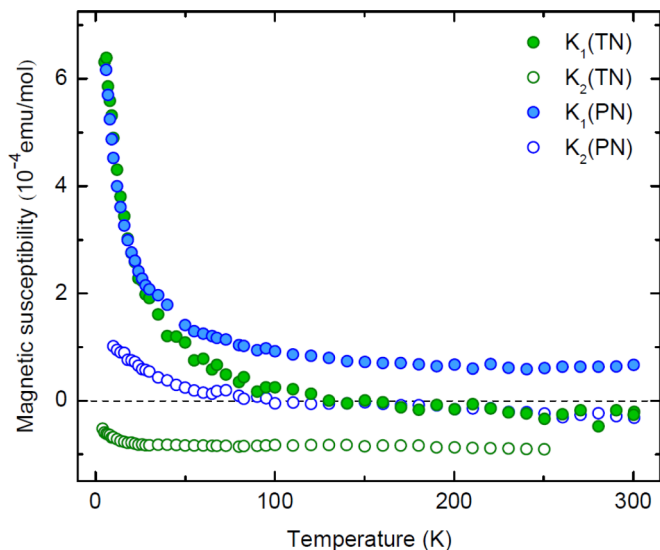


FIG. 3. Temperature dependence of the magnetic susceptibilities of  $K_1(\text{TN})$  (filled green circles),  $K_2(\text{TN})$  (empty green circles),  $K_1(\text{PN})$  (filled blue circles), and  $K_2(\text{PN})$  (empty blue circles).

instability accompanied by a decrease in crystal symmetry, resulting in dimer formation between adjacent molecules as  $[\text{K}^+(\text{PLA})^-]_2$ . In the latter case, the LUMO-derived band splits into lower singlet and higher triplet states due to the spin-exchange interactions, and a small energy gap opens. The spin singlet ground states with an energy gap resulting from  $[\text{K}^+(\text{PLA})^-]_2$  can also explain the observed small magnetic susceptibilities for  $K_1(\text{TN})$  and  $K_1(\text{PN})$ .

In order to determine experimentally which scenario is correct, we directly prepared divalent  $K_2(\text{TN})$  and  $K_2(\text{PN})$  and their XRD profiles (see the Supplemental Material in Ref. [28]) as well as their physical properties were compared with those of the nominal  $K_1(\text{TN})$  and  $K_1(\text{PN})$ . As seen in Fig. 3, the temperature evolution of  $\chi$  for both  $K_1(\text{TN})$  and  $K_1(\text{PN})$  was significantly different from those of  $K_2(\text{TN})$  and  $K_2(\text{PN})$ , respectively. From these experiments, one can know that although the divalent  $K_2(\text{TN})$  and  $K_2(\text{PN})$  phases are stable, they are markedly different from the electronic states of  $K_1(\text{TN})$  and  $K_1(\text{PN})$  synthesized from the 1:1 nominal composition. This is more firmly discussed by optical measurements later. Consequently, the first scenario for the small  $n$  observed in  $K_1(\text{TN})$  and  $K_1(\text{PN})$  can safely be ruled out, and the latter scenario in terms of the spin Peierls instability leading to a dimer of adjacent molecules with the singlet ground states can be a more likely explanation.

### B. Optical spectroscopy

In the optical reflectance spectra of  $K_1(\text{PLAs})$ , the emergence of the LUMO + 1 excitation from the LUMO at 1 to 2 eV was similar to the observations previously reported for free solvated anions [29]. These observations clearly indicate that their LUMO-derived bands are occupied by electrons in the ground states. The adsorption tails are clearly observed in the near-infrared region, and the Drude term originating from itinerant carriers was not observed. Therefore, we can conclude that all  $K_1(\text{NN})$ ,  $K_1(\text{AN})$ ,  $K_1(\text{TN})$ , and  $K_1(\text{PN})$  are

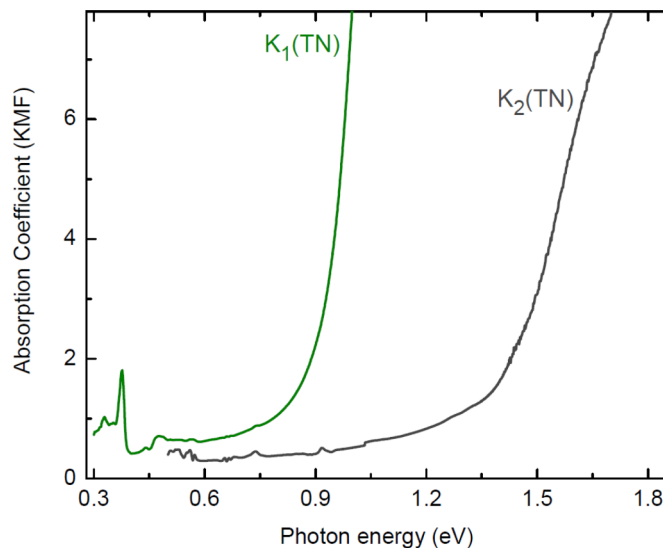


FIG. 4. Absorption spectra of  $K_1(\text{TN})$  and  $K_2(\text{TN})$ .

insulators, although the reason is different between the former two and the latter two compounds as described earlier.

In order to investigate the differences between  $K_1(\text{TN/PN})$  and  $K_2(\text{TN/PN})$ , we directly compared the optical spectra of their  $K_1$  and  $K_2$  phases. Figure 4 shows the absorption spectra of  $K_1(\text{TN})$  and  $K_2(\text{TN})$  in which sharp absorption edge was observed for both  $K_1(\text{TN})$  and  $K_2(\text{TN})$ . Similar results were also obtained in  $K_1(\text{PN})$  and  $K_2(\text{PN})$ . An important conclusion of these optical experiments is that the extremely small magnetic susceptibilities observed for both  $K_1(\text{TN/PN})$  and  $K_2(\text{TN/PN})$  phases are insulator and stable in the TN and the PN systems. In  $K_2(\text{TN/PN})$  case, the insulating ground states can be assumed as the consequence of a fully occupied LUMO-derived band in a simple band filling picture. As for  $K_1(\text{TN/PN})$ , the second scenario of a dimer  $[(\text{PLA})^-]_2$  formation is reasonable. In the following paragraph unambiguous evidence additionally obtained from Raman spectroscopic experiments is described.

### C. Raman spectroscopy

Room-temperature Raman spectra of pristine PLAs and their K-intercalated compounds with the 1:1 stoichiometry were measured. Figure 5 shows the Raman spectra of pristine NN and  $K_1(\text{NN})$  together with that of pristine AN and  $K_1(\text{AN})$ . Both NN and AN molecules belong to the  $D_{2h}$  point group, and therefore 24 and 32 Raman-active vibration modes, respectively, can be expected from the symmetry considerations [30]. Experimentally, however, a smaller number of Raman-active modes was observed for both pristine NN and pristine AN, which is similar to the previous experimental results for powder samples [31]. Similarly for  $K_1(\text{AN})$ , almost all peaks of  $K_1(\text{NN})$  shifted to the lower wave numbers than those of pristine NN. The observed phonon softening is caused by the occupation of electrons in the antibonding orbital, indicating that electrons transfer from K to a LUMO-derived band of antibonding orbitals in NN or AN.

In the case of TN, the Raman spectrum well agrees with that in the previous report [32]. The vibrations were reasonably

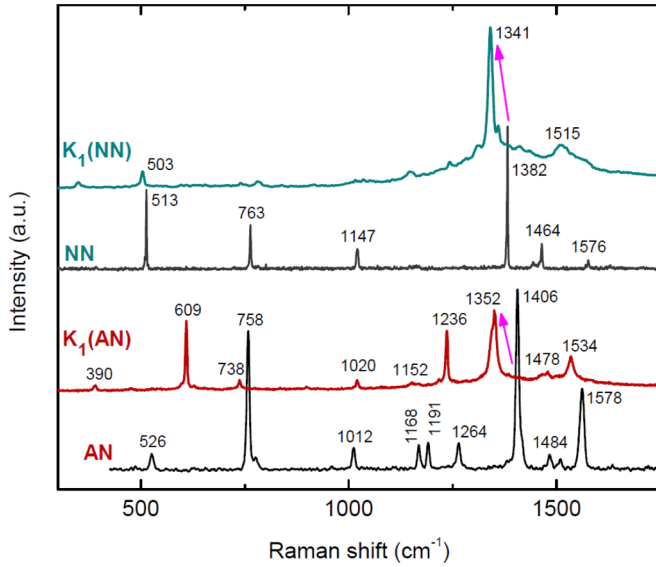


FIG. 5. Room-temperature Raman spectra of pristine NN,  $K_1$ (NN), AN, and  $K_1$ (AN).

assigned to the stretching and the bending modes of C-C and C-H. Almost all vibration modes of  $K_1$ (TN) and  $K_2$ (TN) shifted to the lower wave numbers than those of pristine TN as shown in Fig. 6, the lattice softening of which is due to the electron transfer from K to TN as was discussed earlier for NN. In addition, the remarkably distinguishable Raman spectra between  $K_1$ (TN) and  $K_2$ (TN) indicate that their ground states are markedly different from each other in structural symmetry. This is unambiguous experimental evidence to rule out the first scenario for explaining the small  $n$  observed for  $K_1$ (TN) and  $K_1$ (PN). In particular, a remarkable difference was the fact that the Raman spectrum of  $K_1$ (TN) exhibits not only the shift, but also many new peaks that are not present in pristine TN. These experimental observations support our

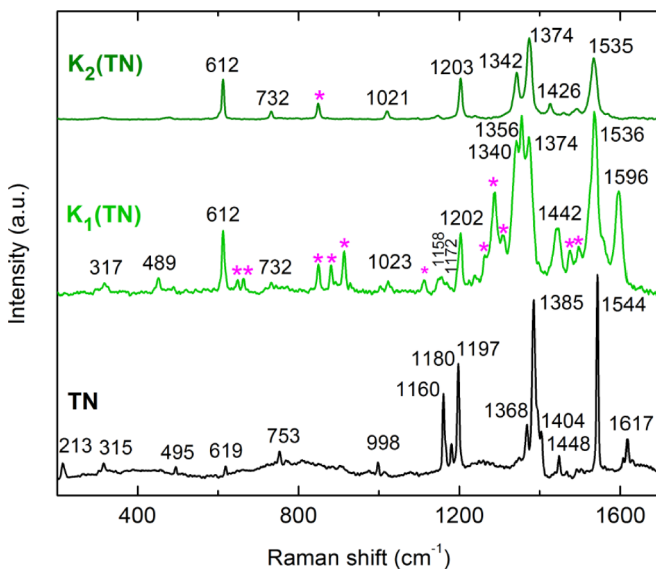


FIG. 6. Room-temperature Raman spectra of pristine TN,  $K_1$ (TN), and  $K_2$ (TN). The pink asterisks show the new peak positions.

interpretation described earlier that the molecular symmetry reduces in leading to dimerization of the  $K_1$ (TN) units as a consequence of the Peierls instability.

#### D. First-principles calculations

Our experiments indicate that the ground states of  $K_1$ (NN) and  $K_1$ (AN) are Mott insulators, whereas those of  $K_1$ (TN) and  $K_1$ (PN) are, in contrast, band insulators via dimer formation with singlet ground states caused by spin Peierls instability. The ground states are different between the NN/AN group in the monoclinic crystal system (space group of  $P2_1/a$ ) [33,34] and the TN/PN group of the triclinic crystal system (space group of  $P-1$ ) [35,36]. The reason for this classification into two groups is not immediately clear, and therefore we made first-principles calculations for understanding the present results. Figure 7 shows the potential-energy profiles as a function of center-to-center molecular distance of  $[(PLA)^-]_2$  evaluated by the *ab initio* calculations. Here, we consider the herringbone stacking configurations extracted from the pristine PLA crystals since the intermolecular interactions of the herringbone configurations are stronger than those of parallel configurations. Our calculations clearly indicate that the binding energies of PLA dimers become larger as the number of benzene rings increases. The energy gain obtained by the large intermolecular interactions of TN and PN is favorable for the dimer formation, and thus this trend is consistent with the experimental observations.

We further theoretically investigated the bond order of  $[(PLA)^-]_2$  as well as the excitation energy from the singlet ground state ( $S_0$ ) to the triplet state ( $T_1$ ), i.e., the spin-flip energy as shown in Fig. 8. We employed the dimer configurations of the pristine crystals for the present calculations. Both bond order and spin-flip energy increase systematically as the PLA molecule becomes larger, indicating that the electronic states change from the Mott insulating states for

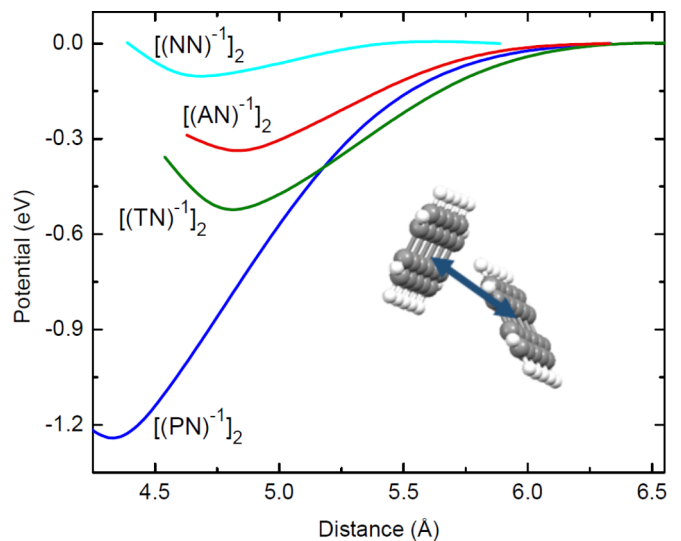


FIG. 7. Potential-energy profile as a function of center-to-center distance of the PLA dimer by the MRMP2 calculations with the triple- $\zeta$  basis set and the SBKJC pseudopotential where the active space consists of the highest occupied molecular orbital (HOMO) and LUMO orbitals of the dimer.

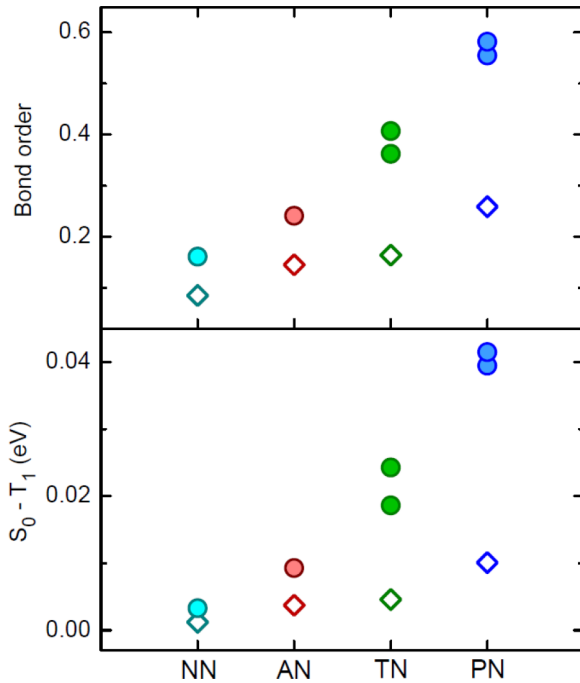


FIG. 8. Bond order (upper panel) and spin-flip energy (lower panel) of PLA dimers by the MRMP2 calculations. The filled circles and empty marks present for the herringbone and parallel configurations, respectively, where TN and PN have two distinguishable herringbone configurations. The bond order is defined by the difference in natural populations of the bonding (HOMO) and antibonding (LUMO) orbitals of dimer, which is multiplied by the factor of 0.5 and takes a value from 0 to 1.

AN and NN to the band insulating states via dimerization for TN and PN. Although the intermolecular interactions are considerably different between the two distinguishable herringbone configurations in TN and PN, such a difference is not evident in AN and NN. Intriguingly to be emphasized is a fact that the herringbone packing of the PLA crystal forms a triangular lattice of the doped spins with spin frustration. The anisotropic intermolecular interactions of the herringbone configurations in TN and PN seem to eliminate the spin frustration via the formation of a dimer accompanied by lower geometrical symmetry. In the AN and NN crystals, such lower symmetry is unfavored, and a similar spin frustration would oppositely stabilize the Mott insulating states.

As described above, the ground states of PLA systems with a half-filled band are strongly affected by the number of benzene rings as well as the crystal symmetry. Figure 9 shows various electronic phases and schematic crystal models in electron-doped PLAs. In particular, the metallic phase which Akamatsu *et al.* dreamed in 1954 can be expected as a high-pressure phase of Mott insulators [1]. In the hole-doped system  $I_1(\text{PN})$ , a biradical (dimer) state showing thermal spin excitation from a singlet ground state to an accessible triplet state was suggested previously from its temperature dependence of magnetic susceptibility [23]. The present experimental observations of a dimer with singlet ground state via one-electron transfer to TN or PN are high accuracy results in the electron-doped system. However in the present

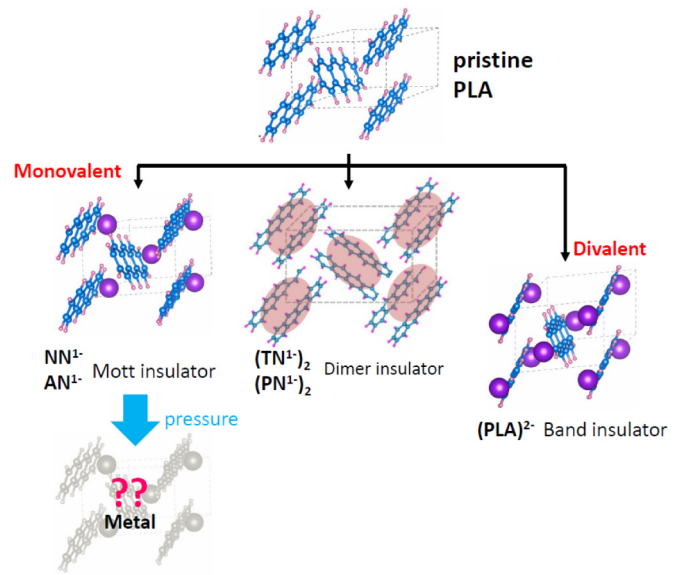


FIG. 9. Various possible electronic phases and schematic crystal models in K-intercalated PLAs.

experiments, no signals associated with the thermal accessible triplet states were detected by electron spin resonance in the temperature range from 4 to 300 K, and this is most probably due to the large energy separation of such a triplet state away from the singlet ground state. Our theoretical calculations indicated that the energy separation is larger than 40 meV, which is not accessible at room temperature. It is also noted that the Mott insulating state previously suggested in thin films of alkali-metal-doped TN/PN [19–22] is greatly contradictory to the present results. If such a Mott insulating state could exist, this would most likely be caused by the special effects of molecular orientations controlled by the surface interactions between a substrate and the molecules, which may stabilize the Mott insulating state in alkali-metal-doped TN/PN thin films by preventing the Peierls instability.

#### IV. SUMMARY

Focusing on the half-filled band states, K-intercalated PLAs were prepared, and their electronic ground states were studied. Due to the large  $U$  and the small  $W$ , the ground states of the two smallest PLAs (NN and AN) were determined to be Mott insulators. On the other hand, such a criterion was changed when the number of benzene rings increased to the larger TN and PN. The electronic states of the larger number of PLAs intercalated with the 1:1 stoichiometry showed spin Peierls instability leading to dimer formation between adjacent molecules. These results were unambiguously confirmed by optical and vibrational spectroscopic data as well as magnetic susceptibilities in addition to the crystal structural information. Considering the present results of the four PLAs intercalated with K, a dimer insulator seems to be more stable in a half-filled band when the number of benzene rings increases. These experimental results suggest that several routes to insulating are actually possible by a sensitive balance between electron correlations and flexible deformation in molecular solids. This was supported by first-principles calculations. It will be

interesting to see in the future whether this prediction can be correct for other extended systems in PLAs and the dreamed metallic phase can be detected.

#### ACKNOWLEDGMENTS

This work was supported by the Scientific Research Fund, the World Premier International Research Center Initiative

(WPI) from the Ministry of Education, Culture, Sports, Science and Technology (MEXT) of Japan, and the Tohoku University GCOE program. This work was also supported by the Joint Studies Program: No. 252 and No. 630 of the Institute for Molecular Science and by the Nanotechnology Platform Program: No. B107, No. S-13-MS-0004, No. S-13-MS-1041, and No. S-14-MS-1046 (Molecule and Material Synthesis) of MEXT and a Grant in Aid for Scientific Research (Grant No. 15K17690).

- 
- [1] H. Akamatu, H. Inokuchi, and Y. Matsunaga, *Nature (London)* **173**, 168 (1954).
- [2] R. Mitsuhashi, Y. Suzuki, Y. Yamanari, H. Mitamura, T. Kambe, N. Ikeda, H. Okamoto, A. Fujiwara, M. Yamaji, N. Kawasakiv, and Y. Kubozono, *Nature (London)* **464**, 76 (2010).
- [3] X. F. Wang, R. H. Liu, Z. Gui, Y. L. Xie, Y. J. Yan, J. J. Ying, X. G. Luo, and X. H. Chen, *Nat. Commun.* **2**, 507 (2011).
- [4] X. F. Wang, Y. J. Yan, Z. Gui, R. H. Liu, J. J. Ying, X. G. Luo, and X. H. Chen, *Phys. Rev. B* **84**, 214523 (2011).
- [5] X. F. Wang, X. G. Luo, J. J. Ying, Z. J. Xiang, S. L. Zhang, R. R. Zhang, Y. H. Zhang, Y. J. Yan, A. F. Wang, P. Cheng, and X. H. Chen, *J. Phys.: Condens. Matter* **24**, 345701 (2012).
- [6] T. Kosugi, T. Miyake, S. Ishibashi, R. Arita, and H. Aoki, *Phys. Rev. B* **84**, 214506 (2011).
- [7] T. Kato, T. Kambe, and Y. Kubozono, *Phys. Rev. Lett.* **107**, 077001 (2011).
- [8] G. Giovannetti and M. Capone, *Phys. Rev. B* **83**, 134508 (2011).
- [9] M. Kim, B. I. Min, G. Lee, H. J. Kwon, Y. M. Rhee, and J. H. Shim, *Phys. Rev. B* **83**, 214510 (2011).
- [10] P. L. de Andres, A. Guijarro, and J. A. Vergés, *Phys. Rev. B* **83**, 245113 (2011).
- [11] H. Okazaki, T. Wakita, T. Muro, Y. Kaji, X. Lee, H. Mitamura, N. Kawasaki, Y. Kubozono, Y. Yamanari, T. Kambe, T. Kato, M. Hirai, Y. Muraoka, and T. Yokoya, *Phys. Rev. B* **82**, 195114 (2010).
- [12] M. Casula, M. Calandra, G. Profeta, and F. Mauri, *Phys. Rev. Lett.* **107**, 137006 (2011).
- [13] M. Cuputo, D. G. Santo, P. Parisse, L. Petaccia, L. Floreano, A. Verdini, M. Panighe, C. Struzzi, B. Taleatu, C. Lal, and A. Goldoni, *J. Phys. Chem. C* **116**, 19902 (2012).
- [14] B. Mahns, F. Roth, and M. Knupfer, *J. Chem. Phys.* **136**, 134503 (2012).
- [15] A. Ruff, M. Sing, R. Claessen, H. Lee, M. Tomić, H. O. Jeschke, and R. Valentí, *Phys. Rev. Lett.* **110**, 216403 (2013).
- [16] S. Heguri, Q. Thi Nhu Phan, Y. Tanabe, and K. Tanigaki, *Phys. Rev. B* **90**, 134519 (2014).
- [17] S. Heguri, M. Kobayashi, and K. Tanigaki, *Phys. Rev. B* **92**, 014502 (2015).
- [18] Y. C. Cheng, R. J. Silbey, D. A. da Silva Filho, J. P. Calbert, J. Cornil, and J. L. Bredas, *J. Chem. Phys.* **118**, 3764 (2003).
- [19] M. F. Craciun, G. Giovannetti, S. Rogge, G. Brocks, A. F. Morpurgo, and J. van den Brink, *Phys. Rev. B* **79**, 125116 (2009).
- [20] E. Annese, J. Fujii, I. Vobornik, and G. Rossi, *J. Phys. Chem.* **116**, 2382 (2012).
- [21] F. Bussolotti, S. Kera, and N. Ueno, *Phys. Rev. B* **86**, 155120 (2012).
- [22] F. Roth and M. Knupfer, *J. Chem. Phys.* **143**, 154708 (2015).
- [23] M. Brinkmann, V. S. Videva, A. Bieber, J. J. Andre, P. Turek, L. Zuppiroli, P. Bugnon, M. Schaer, F. Nuesch, and R. Humphry-Baker, *J. Phys. Chem. A* **108**, 8170 (2004).
- [24] Q. T. N. Phan, S. Heguri, Y. Tanabe, H. Shimotani, T. Nakano, Y. Nozue, and K. Tanigaki, *Dalton Trans.* **43**, 10040 (2014).
- [25] Q. T. N. Phan, S. Heguri, Y. Tanabe, H. Shimotani, and K. Tanigaki, *Eur. J. Inorg. Chem.* **2014**, 4033 (2014).
- [26] M. W. Schmidt, K. K. Baldrige, J. A. Boatz, S. T. Elbert, M. S. Gordon, J. H. Jensen, S. Koseki, N. Matsunaga, K. A. Nguyen, S. Su, T. L. Windus, M. Dupuis, and J. A. Montgomery, *J. Comput. Chem.* **14**, 1347 (1993).
- [27] Y. Iwasa and T. Takenobu, *J. Phys.: Condens. Matter* **15**, R495 (2003).
- [28] See Supplemental Material at <http://link.aps.org/supplemental/10.1103/PhysRevB.93.075130> for details of the XRD profiles for  $K_x$ (PLAs).
- [29] K. H. J. Buschow and G. J. Hoijtink, *J. Chem. Phys.* **40**, 2501 (2004).
- [30] J. Räsänen, F. Stenman, and E. Penttinen, *Spectrochim. Acta, Part A* **29**, 395 (1973).
- [31] F. Stenman, *J. Chem. Phys.* **54**, 4217 (2003).
- [32] A. I. Alajtal, H. G. M. Edwards, M. A. Elbagerma, and I. J. Scowen, *Spectrochim. Acta, Part A* **76**, 1 (2010).
- [33] D. Cruickshank, *Acta Crystallogr.* **10**, 504 (1957).
- [34] A. Charlesby, G. Finch, and H. Wilman, *Proc. Phys. Soc., London* **51**, 479 (1939).
- [35] J. M. Robertson, V. Sinclair, and J. Trotter, *Acta Crystallogr.* **14**, 697 (1961).
- [36] C. C. Mattheus, A. B. Dros, J. Baas, A. Meetsma, J. L. de Boer, and T. T. M. Palstra, *Acta Crystallogr., Sect. C: Cryst. Struct. Commun.* **57**, 939 (2001).